



Predicting Fractures Using Vertebral ^{18}F -NaF Uptake in Prostate Cancer Patients

Helene Chesnais, Nikita Bastin, Sofia Miguez, Daniel Kargilis, Anita Kalluri, Ashley Terry, Chamith S. Rajapakse

Department of Radiology, University of Pennsylvania, Philadelphia, PA, USA

Corresponding author

Helene Chesnais

Department of Radiology, University of Pennsylvania, 1 Founders Pavilion, 3400 Spruce St. Philadelphia, PA 19104, USA
Tel: +1-646-436-6590
Fax: +1-215-662-7263
E-mail: helene.chesnais@gmail.com

Received: August 1, 2023

Revised: October 1, 2023

Accepted: October 8, 2023

This study has been presented at the 2021 Annual Meeting of the American Society for Bone and Mineral Research (ASBMR), San Diego, CA, USA (Oct. 1-4, 2021).

Copyright © 2023 The Korean Society for Bone and Mineral Research

This is an Open Access article distributed under the terms of the Creative Commons Attribution Non-Commercial License (<https://creativecommons.org/licenses/by-nc/4.0/>) which permits unrestricted non-commercial use, distribution, and reproduction in any medium, provided the original work is properly cited.



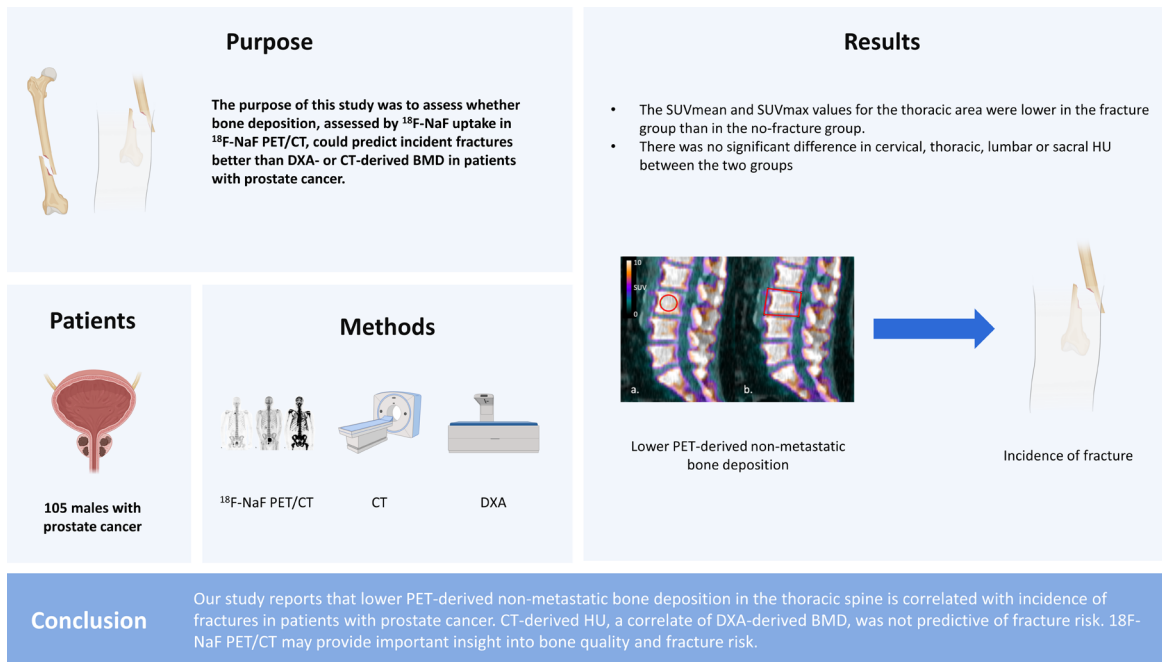
Background: Patients with prostate cancer tend to be at heightened risk for fracture due to bone metastases and treatment with androgen-deprivation therapy. Bone mineral density (BMD) derived from dual energy X-ray absorptiometry (DXA) is the standard for determining fracture risk in this population. However, BMD often fails to predict many osteoporotic fractures. Patients with prostate cancer also undergo ^{18}F -sodium fluoride (^{18}F -NaF)-positron emission tomography/computed tomography (PET/CT) to monitor metastases. The purpose of this study was to assess whether bone deposition, assessed by ^{18}F -NaF uptake in ^{18}F -NaF PET/CT, could predict incident fractures better than DXA- or CT-derived BMD in patients with prostate cancer. **Methods:** This study included 105 males with prostate cancer who had undergone full body ^{18}F -NaF PET/CT. Standardized uptake value (SUVmean and SUVmax) and CT-derived Hounsfield units (HU), a correlate of BMD, were recorded for each vertebral body. The average SUVmean, SUVmax, and HU were calculated for cervical, thoracic, lumbar, and sacral areas. The *t*-test was used to assess significant differences between fracture and no-fracture groups. **Results:** The SUVmean and SUVmax values for the thoracic area were lower in the fracture group than in the no-fracture group. There was no significant difference in cervical, thoracic, lumbar or sacral HU between the 2 groups. **Conclusions:** Our study reports that lower PET-derived non-metastatic bone deposition in the thoracic spine is correlated with incidence of fractures in patients with prostate cancer. CT-derived HU, a correlate of DXA-derived BMD, was not predictive of fracture risk. ^{18}F -NaF PET/CT may provide important insight into bone quality and fracture risk.

Key Words: Fractures, bone · Positron emission tomography computed tomography · Prostatic neoplasms · Spine

INTRODUCTION

In patients with prostate cancer, bone is a dominant site of metastasis.[1] Bone metastases often lead to bone mineral density (BMD) decreases, bone fractures, spinal cord compression, and pain. In addition to bone metastases, other primary contributors to bone fragility in prostate cancer patients include aging-related bone loss as well as androgen-deprivation therapy (ADT), which increases the risk of osteopenia, osteoporosis, and fractures.[2,3] Osteoporosis is present in up to 42% of prostate cancer patients even before they start ADT.[4] Prostate cancer patients receiving ADT have been reported to experience BMD losses in the lumbar spine, total hip, and femoral neck, contributing to the diagnosis of osteoporosis.[4] Bone loss and osteoporosis greatly increase the risk of sustaining debilitating frac-

Graphical Abstract



tures; thus, fracture prevention is a major concern in prostate cancer patients.[5]

BMD derived from dual energy X-ray absorptiometry (DXA), often combined with a fracture risk assessment tool (FRAX) score, is the standard of care for determining fracture risk. While BMD and BMD T-score are used to determine bone strength, the role of FRAX in determining fracture risk in patients with cancer-associated bone disease has not been standardized.[6] FRAX does not account for the effect of malignancy and treatment on fracture risk. There is a need for additional diagnostic measures to assess for fracture risk in prostate cancer patients.

The ^{18}F sodium fluoride (^{18}F -NaF) is an U.S. Food and Drug Administration-approved radiotracer for monitoring metastatic bone disease using positron emission tomography/computed tomography (PET/CT).[7-9] ^{18}F -NaF PET/CT is currently used to evaluate both disease progression in the bone and response to prostate cancer treatment [10,11]; simultaneously, it functions as a powerful tool to study bone formation and healing from fracture.[12-14] Recently, ^{18}F -NaF PET/CT has been shown to be useful in detecting age-related changes in bone metabolism.[15,16] Since fracture strength of metastatic bone depends on the lesion loca-

tion,[17] the ability to assess localized bone metabolism could provide information not captured by global imaging markers. However, the application of ^{18}F -NaF PET/CT markers in assessing fracture risk in prostate cancer patients is not well established. Therefore, it would be useful to investigate the potential for opportunistic osteoporosis assessment and fracture risk reduction with PET/CT.[15,18-21]

The purpose of this study was to assess whether bone deposition, assessed by ^{18}F -NaF uptake in ^{18}F -NaF PET/CT scans, could predict incident fractures better than DXA- or CT-derived BMD in prostate cancer patients.

METHODS

1. Data collection

This retrospective study utilized clinical data from patients of our institution's healthcare system. The study protocol was approved by the Institutional Review Board and exempted from continuing review. Written consent was not obtained from patients as all data was de-identified.

The study included patients with a history of prostate cancer who had undergone ^{18}F -NaF PET/CT imaging. The 112 male patients were identified as having full-body ^{18}F -

NaF PET/CT scans available for image analysis. Criteria for inclusion were male sex, availability of ^{18}F -NaF, and diagnosis of prostate cancer. Criteria for exclusion were extensive spinal metastases (4 patients), SUVmean and SUVmax values less than 2 standard deviations from the mean (1 patient), or corrupted PET/CT images (2 patients). Of the initial 112 patients with imaging, 105 patients (ages, 53–91 years; mean age, 70.8; mean body mass index [BMI], 29.2 kg/m²) met these criteria and were retained in the study.

The data sampling time was from January 2012 to December 2019. Demographic, cancer therapy and fracture information were obtained from electronic medical records, whereas ^{18}F -NaF PET/CT and DXA data were obtained from radiological records.

Each patient chart was searched thoroughly for the incidence of clinical fractures subsequent to the scan. The keywords “fracture”, “fx”, “frax”, “osteoporotic fracture”, “break”, and “compression” were used. All body fractures were recorded and subsequently categorized by location: spine, ribs, hip, arm, leg, and foot bones. The time of fracture(s) relative to PET/CT date was recorded.

2. Imaging acquisition

^{18}F -NaF PET/CT images were obtained 66.0 (60.0–74.7) min after intravenous injection of 8.6 (5.4–10.5) mCi ^{18}F -NaF, both reported as median (interquartile range).

3. Image analysis

A PET/CT image processor (Fiji PET/CT Viewer Plug-in, Beth Israel) was used to measure ^{18}F -NaF standardized uptake values (SUVmean and SUVmax) of each vertebra from C2 to S1 in a single-slice rectangular region of interest (ROI) outlining the vertebral body at the midline sagittal view. The midline was determined by selecting the slice where the spinous processes were at their largest in the sagittal view. As a quality control measure, SUVmean and SUVmax were also measured in a spherical ROI at the center of the vertebra, with a 10 mm diameter for all vertebrae except for T12-L5, where a 20 mm diameter was more suited to the larger volume (Fig. 1). Within the rectangular ROI, SUVpeak (the SUVmean in a 1 cc volume centered on SUVmax) and SUVqpeak (the average of SUVmax together with the 3 hottest pixels in a 1 cc volume, centered on SUVmax) were obtained to reduce the statistical fluctuation of a single pixel SUVmax. CT-derived Hounsfield units (HUs) were also

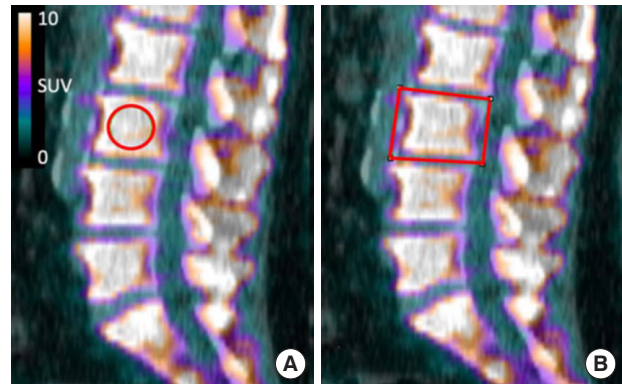


Fig. 1. Example of standardized uptake value (SUV) measurements at L3 with (A) spherical and (B) rectangular volume of interest.

obtained via the rectangular ROI. Throughout the paper, R and S will be used to reference measures obtained with a rectangular and spherical ROI, respectively.

Care was taken to avoid areas of metastases as identified using radiologist reports. In cases where metastases could not be avoided, the vertebra was omitted from the analysis. A total of 34 vertebrae were omitted across all patients. Several omissions came from the same patient in cases with extensive but avoidable metastases in the spine.

Average cervical, thoracic, lumbar, sacral, and spinal SUVmean, SUVmax, SUVpeak, SUVqpeak, and HU were calculated for each participant. The first cervical vertebra and lower sacral vertebrae (S2 and below) were not differentiable on the scans, therefore C2-C7 and S1 values were used to assess cervical and sacral spines, respectively.

4. Statistical analysis

T-tests were used to determine the difference in cervical, thoracic, lumbar, sacral, and average ^{18}F -NaF uptake (SUVmean, SUVmax, SUVpeak, and SUVqpeak) between 2 groups: a group which developed an incident fracture (after their scan) anywhere in the body, and another group which did not. CT-derived HU measures have previously been shown to correlate with clinical standard DXA BMD.[22–25] Average baseline HU measurements were also compared between the fracture vs. no-fracture groups.

Participants were also divided by the incidence or non-incidence of compression fractures in the spine, as opposed to fractures anywhere in the body. HU values were compared with *t*-tests between these 2 groups.

Age, BMI, time to scan and tracer dose were also com-

pared between the 2 groups, looking at all fractures or compression fractures. For patients who underwent DXA, baseline BMD, BMD T-Score, average SUVmean and SUVmax were compared amongst groups with and without fractures using *t*-tests.

5. Reproducibility study

A reproducibility study was conducted between 4 independent operators using rectangular and spherical sampling methods at L3. Mean coefficients of variation (CVs) were calculated for SUVmean and SUVmax in each method.

RESULTS

1. Cohort characteristics and fracture data

Of the initial 112 patients with full body scans, 4 patients were excluded from the analysis due to extensive metastases in the spine that could not be avoided during segmentation, and 1 patient was excluded due to exceptionally low uptake (spine SUVmean, SUVmax, SUVpeak and SUVqpeak measures less than 2 standard deviations from the rest of the cohort) (Fig. 2). Two patients had scans that could not be opened by the imaging software. The total number of patients included in the study was therefore 105. Patient illness and treatment information is detailed in Table 1.

Twenty-seven out of the 105 patients reported at least one bone fracture after the ^{18}F -NaF PET/CT scan (Table 2). Some patients had multiple incident fractures. The major fractures were compression fractures of the spine (N=14), rib fractures (N=8), hip/femur fractures (N=6), and long

bones (N=6). The mean (standard deviation) time between the PET/CT scan and the fracture was 3.1 years (2.5).

2. Deposition and HU

Thoracic SUVmean (in rectangular ROI, R, and spherical ROI, S), SUVmax (R, S), SUVpeak (R), and SUVqpeak (R) were all lower in the group with incident fractures (at least one fracture, anywhere in the body) than in the no-fracture group ($P < 0.05$ for all). Thoracic HU (R) was not different between the 2 groups ($P = 0.3708$). After accounting for differences in administered tracer dose, ^{18}F -NaF uptake in the thoracic spine remained significantly lower in the fracture group (Table 3), in all measures except for thoracic SUVmax (S). Age, BMI, time to scan were not different between the 2 groups. Cervical, lumbar, and sacral ^{18}F -NaF uptake and HU were also not different between the 2 groups.

When combining all vertebrae, there was a significant difference in total spine SUVmean (R, S), SUVmax (R, S), SUVpeak (R), and SUVqpeak (R), ($P < 0.05$ for all) with no difference in spine HU ($P = 0.087$). This difference in spine SUV disappeared when correcting for dose.

An analysis considering only future compression fractures (14 patients) yielded similar results as above. Thoracic and whole spine ^{18}F -NaF were again lower in the compression group but the significance disappeared after correction for dose. One difference was that HU of the spine was lower in patients who developed incident compression fractures (Table 4). Lower HU was observed in the cervical and sacral spine of patients with future compression fractures but not in the thoracic and lumbar regions.



Fig. 2. Example of excluded patients due to (A) insufficient tracer uptake in the spine or (C) extensive spine metastases, compared with (B) a patient with normal tracer uptake.

Table 1. Illness information for participants (N=105), including metastatic status and therapy type

Variables	N	Treatment start date/ radiation end date/ surgery date (yr)
Cancer type		
Metastatic	51	
Non-metastatic	54	
Hormone therapy		
Yes	42	2.1 ± 2.8 ^{a)}
No	47	
Unspecified	16	
Drug name (brand name)		
Androgen deprivation therapy		
Leuprolide (Lupron, Eligard)	32	
Degarelix (Firmagon)	2	
Anti androgens		
Bicalutamide (Casodex)	23	
Nilutamide (Nilandron)	1	
Enzalutamide (Xtandi)	4	
Triple androgen blockade		
Dutasteride (Avodart)	2	
Bone health		
Denosumab (Xgeva)	3	
Radiation therapy		
Yes	45	6.9 ± 5.1 ^{b)}
No	48	
Unspecified	12	
Radiation type		
External beam radiation therapy	12	
Brachytherapy	6	
Intensity-modulated radiation therapy	6	
Salvage radiation therapy	6	
Unspecified	15	
Radical prostatectomy		
Yes	43	7.0 ± 6.3 ^{b)}
No	52	
Unspecified	10	

The data is presented as N or mean ± standard deviation.

^{a)}Months prior to positron emission tomography/computed tomography scan.

^{b)}Years prior to positron emission tomography/computed tomography scan.

3. DXA

Of the 105 patients in the final cohort, 40 also had DXA scans on file. Of those, 13 patients with DXA scans had fractures. DXA characteristics are described in Table 5. Lumbar BMD, BMD T-score, and BMD Z-score were not correlated with the incidence of fractures or compression fractures.

Table 2. Fracture characteristics for the 27 patients with incident fractures

Fracture location	N ^{a)}	Time to fracture (yr)	Description
Spine	14	2.9	T2, T3, T4, T5, T7 (3), midthoracic, T8, T9, T10, T11, T12, L1, L2 (2), L3 (2), L1-4 transverse processes, L2-L3, hemisacrum, unspecified
Rib	8	2.1	
Hip	6	4.2	
Arm/Leg/Foot	6	4.0	

^{a)}The number of total fractures=34. Some patients have multiple fractures.

Table 3. Difference between SUVmean, SUVmax, SUVpeak, SUVqpeak, and HU of the thoracic spine in the fracture vs. no-fracture groups

	Fracture (N=27)	No fracture (N=78)	P-value	Dose-corrected P-value
Thoracic SUVmean (R)	5.2 ± 0.7	5.7 ± 1.3	0.0192	0.0429
Thoracic SUVmean (S)	6.6 ± 1.2	7.3 ± 1.7	0.0215	0.0420
Thoracic SUVmax (R)	8.6 ± 2.1	9.9 ± 2.8	0.0136	0.0204
Thoracic SUVmax (S)	7.9 ± 1.7	8.8 ± 2.2	0.0364	0.0563
Thoracic SUVpeak (R)	7.3 ± 1.4	8.3 ± 2.1	0.0083	0.0163
Thoracic SUVqpeak (R)	7.9 ± 1.8	9.1 ± 2.4	0.0111	0.0170
Thoracic HU (R)	168.6 ± 33.7	175.9 ± 39.7	0.3708	-
Age ^{a)}	71.7 ± 8.1	70.5 ± 7.9	0.4944	-
BMI ^{a)}	29.8 ± 5.3	29.0 ± 5.1	0.5372	-
Minutes to scan ^{a)}	68.1 ± 12.7	69.5 ± 14.3	0.6522	-
Radiotracer dose ^{a)}	8.2 ± 2.7	7.9 ± 2.4	0.5345	-

^{a)}Age, BMI, time to scan, and tracer dosage were not significantly different between the fracture and no-fracture groups.

SUVmean, mean standardized uptake value; R, rectangular region of interest; S, spherical region of interest; SUVmax, maximum standardized uptake value; SUVpeak, peak standardized uptake value; SUVqpeak, the average of SUVmax together with the 3 hottest pixels in a 1 cc volume, centered on SUVmax; HU, Hounsfield units; BMI, body mass index.

4. Reproducibility study

The mean CVs of the 3 dimensional (D) sphere reproducibility study were 4.6% and 3.3%, for SUVmax and SUVmean, respectively, and those for the 2D rectangle study were 6.3% and 4.5%.

DISCUSSION

Our retrospective study reports an appreciably lower thoracic vertebral bone deposition as measured by ¹⁸F-NaF uptake in prostate cancer patients with incident bodily fractures. The lower thoracic bone deposition was associ-

Table 4. Difference in cervical, thoracic, lumbar, and sacral HU between group with incidence of compression fracture (14 out of 105 patients) and no compression fracture

	Compression fracture (N=14)	No compression fracture (N=91)	P-value
Cervical HU (R)	234.1 ± 45.7	283.6 ± 73.9	0.0030
Thoracic HU (R)	160.2 ± 28.9	176.0 ± 39.2	0.0958
Lumbar HU (R)	148.4 ± 30.6	151.3 ± 37.5	0.7673
Sacral HU (R)	146.7 ± 27.4	166.4 ± 45.0	0.0456
Average spine HU	175.9 ± 19.2	198.7 ± 43.2	0.0003
Age ^{a)}	73.4 ± 8.4	70.4 ± 7.8	0.2213
BMI ^{a)}	29.5 ± 6.2	29.2 ± 5.0	0.8408
Minutes to scan ^{a)}	71.1 ± 15.9	68.9 ± 13.6	0.6558
Radiotracer dose ^{a)}	7.9 ± 2.8	7.9 ± 2.5	0.9900

^{a)}Age, BMI, time to scan, and tracer dosage were not significantly different between the fracture and no-fracture groups.

HU, Hounsfield units; R, rectangular region of interest; BMI, body mass index.

ated with fractures but not lower thoracic bone density, suggesting the thoracic spine as a potential area of interest in fracture prediction in prostate cancer patients with access to an ¹⁸F-NaF PET/CT scan. Cervical, lumbar, and sacral ¹⁸F-NaF uptake, as well as age and BMI, were not significantly different in fracture versus no-fracture groups. CT-derived BMD measures were also not different between the 2 groups.

One possible explanation for our findings is that patients who undergo chemotherapy or radiotherapy experience bone loss which not only reduces bone metabolism of the spine but also increases the risk for fracture.[26,27] We observed no significant difference in CT-derived BMD between the fracture and no fracture groups to confirm this. We did see a lower CT-derived BMD in the cervical and sacral regions of 14 patients with incident compression fractures but not in the thoracic or lumbar regions. It is worth noting that CT-derived BMD, measured in HU, is not a perfect correlate to DXA-derived BMD. Yet, in patients who received DXA scans (40 out of 105), BMD and associated markers (T-score and Z-score) were not significantly different in groups with and without incident fractures, suggesting the poor fracture-predictive ability of DXA in this population.

The possibility that a slow-down in the deposition of new bone material precedes bone loss and fractures is also a plausible explanation for the observed differences in bone deposition between the fracture and non-fracture groups despite comparable thoracic CT-derived BMD measures.

Table 5. Information on DXA scans

Variables	N (N=40)	Mean ± SD
Osteoporosis diagnosis		
Normal	18	
Osteopenic	18	
Osteoporotic	4	
DXA characteristics		
BMD (g/cm ²)	38	1.3 ± 0.3
BMD T-score	39	1.2 ± 2.4
FRAX (10-year probability for any major osteoporotic fracture [%])	13	6.7 ± 2.0
Mean months between PET/CT and DXA	39	19.6 ± 24.0

DXA, dual energy X-ray absorptiometry; BMD, bone mineral density; FRAX, fracture risk assessment tool; PET, positron emission tomography; CT, computed tomography; SD, standard deviation.

Vertebral fractures are most common between T8 and L4, [28] which suggests that changes in bone deposition may occur earlier in the thoracic and lumbar spine before affecting other areas of the spine.

The potential confounder of metastasis to bone is an important consideration in interpreting the results of this study. Prostate carcinomas have a propensity to metastasize to the spine, with a decreasing involvement from the lumbar to thoracic to cervical spine hypothesized to be caused by an upward metastatic spread along spinal veins after initial lumbar metastasis. In one study, Amelot et al. [29] found that prostate cancer was associated with L1-L4 and T8 metastases. It has also been noted that pelvic and spinal metastases are most common in patients with fewer lesions, suggesting that such lesions occur early in the disease progression.[30] Bony metastases can increase the uptake of ¹⁸F-NaF. Given the involvement of the lumbar spine in the metastatic progression of the disease, an increase in lumbar ¹⁸F-NaF uptake is expected to correlate with a poorer oncologic prognosis and an increased risk for fractures. This study omitted from analysis all vertebrae with metastases, yet metastatic involvement of the spine could have been missed or invisible on the scans. Undetected metastases could potentially raise ¹⁸F-NaF uptake in the spine, particularly in the lumbar spine, where metastasis is more likely. In addition, such an overestimation would likely be more pronounced in the fracture group due to the demonstrated association between metastasis and fracture. However, the authors of this study consider this effect unlikely because it would not be expected to spare the thoracic spine,

where lower uptake in the fracture group was clearly observed.

Our study has some limitations. We controlled for multiple variables that may influence SUV, such as age, BMI, tracer dose, and uptake period; however, we did not extend this to include other variables of interest, including patient factors such as mobility, blood sugar, or therapy duration, and scanner differences on SUV. While we did not analyze the effect of each therapy on fracture incidence, it is of note that our cohort is sufficiently therapeutically diverse to be representative of the prostate cancer patient population. Other limitations to our study include the retrospective collection of data entailing limited availability of data points near in time to the scan. BMI was especially affected with some time points at a maximum 2 months before or after the scan. Retrospective data collection also limits our characterization of fractures as pathologic, traumatic, or insufficiency fractures, and we did not assess whether fractures occurred at sites of metastasis. Our study's largest limitation was that not all scans were performed on the same scanner and the doses ranged from 5 to 10 mCi approximately. We partially accounted for this difference by adjusting for the effect of the radiotracer dose, but future studies should prospectively standardize the protocol for each patient.

In our pilot study, we retrospectively evaluated fracture risk in prostate cancer patients using ¹⁸F-NaF PET/CT data. We discovered that ¹⁸F-NaF uptake could serve as an indicator of spinal bone deposition, potentially improving fracture prediction compared to existing methods like DXA. Currently, no modality can measure bone turnover rates, but ¹⁸F-NaF scans provide valuable insights into bone metabolism. This information could be clinically beneficial for predicting and preventing fractures, particularly in the context of prostate cancer. Moreover, ¹⁸F-NaF has applications in other medical fields, such as cardiac imaging for cardiovascular health assessment.[31,32] This suggests the possibility of gathering additional information about bone health during ¹⁸F-NaF PET/CT scans in aging populations, although this concept hasn't been studied extensively yet. To advance this research, we propose that future studies explore the combination of ¹⁸F-NaF uptake with approved fracture risk assessment tools to determine its added value in fracture prediction and prevention.

DECLARATIONS

Ethics approval and consent to participate

The study protocol was approved by the Institutional Review Board and exempted from continuing review. Written consent was not obtained from patients as all data was de-identified.

Conflict of interest

No potential conflict of interest relevant to this article was reported.

ORCID

Helene Chesnais <https://orcid.org/0000-0002-3936-726X>
 Nikita Bastin <https://orcid.org/0000-0002-6058-2634>
 Sofia Miguez <https://orcid.org/0000-0003-3912-1996>
 Daniel Kargilis <https://orcid.org/0000-0001-7013-4301>
 Anita Kalluri <https://orcid.org/0000-0002-5783-3877>
 Ashley Terry <https://orcid.org/0000-0001-9800-6598>
 Chamith S. Rajapakse <https://orcid.org/0000-0002-9247-833X>

REFERENCES

1. Chang CH, Tsai CS, Jim YF, et al. Lumbar bone mineral density in prostate cancer patients with bone metastases. *Endocr Res* 2003;29:177-82. <https://doi.org/10.1081/erc-120022298>.
2. Coleman RE, Croucher PI, Padhani AR, et al. Bone metastases. *Nat Rev Dis Primers* 2020;6:83. <https://doi.org/10.1038/s41572-020-00216-3>.
3. Hussain A, Tripathi A, Pieczonka C, et al. Bone health effects of androgen-deprivation therapy and androgen receptor inhibitors in patients with nonmetastatic castration-resistant prostate cancer. *Prostate Cancer Prostatic Dis* 2021;24:290-300. <https://doi.org/10.1038/s41391-020-00296-y>.
4. Tuck SP. Prostate cancer and fracture: Identifying at-risk groups. *J Clin Densitom* 2017;20:196-7. <https://doi.org/10.1016/j.jocd.2016.06.009>.
5. Wallander M, Axelsson KF, Lundh D, et al. Patients with prostate cancer and androgen deprivation therapy have increased risk of fractures—a study from the fractures and fall injuries in the elderly cohort (FRAILCO). *Osteoporos Int* 2019;30:115-25. <https://doi.org/10.1007/s00198-018-4722-3>.

6. Rizzoli R, Body JJ, Brandi ML, et al. Cancer-associated bone disease. *Osteoporos Int* 2013;24:2929-53. <https://doi.org/10.1007/s00198-013-2530-3>.
7. Zhang J, Zhai G, Yang B, et al. Computerized tomography (CT) updates and challenges in diagnosis of bone metastases during prostate cancer. *Curr Med Imaging* 2020;16:565-71. <https://doi.org/10.2174/1573405614666181009144601>.
8. Hardcastle N, Hofman MS, Lee CY, et al. NaF PET/CT for response assessment of prostate cancer bone metastases treated with single fraction stereotactic ablative body radiotherapy. *Radiat Oncol* 2019;14:164. <https://doi.org/10.1186/s13014-019-1359-0>.
9. Velez EM, Desai B, Jadvar H. Treatment response assessment of skeletal metastases in prostate cancer with (18)F-NaF PET/CT. *Nucl Med Mol Imaging* 2019;53:247-52. <https://doi.org/10.1007/s13139-019-00601-1>.
10. Kyriakopoulos CE, Heath EI, Ferrari A, et al. Exploring spatial-temporal changes in (18)F-sodium fluoride PET/CT and circulating tumor cells in metastatic castration-resistant prostate cancer treated with enzalutamide. *J Clin Oncol* 2020;38:3662-71. <https://doi.org/10.1200/jco.20.00348>.
11. Weisman AJ, Harmon SA, Perk TG, et al. Quantification of bone flare on (18)F-NaF PET/CT in metastatic castration-resistant prostate cancer. *Prostate Cancer Prostatic Dis* 2019;22:324-30. <https://doi.org/10.1038/s41391-018-0110-5>.
12. Sanchez-Crespo A, Christiansson F, Thur CK, et al. Predictive value of [(18)F]-fluoride PET for monitoring bone remodeling in patients with orthopedic conditions treated with a Taylor spatial frame. *Eur J Nucl Med Mol Imaging* 2017;44:441-8. <https://doi.org/10.1007/s00259-016-3459-5>.
13. Lundblad H, Karlsson-Thur C, Maguire GQ, Jr., et al. Can Na(18)F PET/CT bone scans help when deciding if early intervention is needed in patients being treated with a TSF attached to the tibia: insights from 41 patients. *Eur J Orthop Surg Traumatol* 2021;31:349-64. <https://doi.org/10.1007/s00590-020-02776-2>.
14. Lundblad H, Karlsson-Thur C, Maguire GQ, Jr., et al. Can spatiotemporal fluoride ((18)F(-)) uptake be used to assess bone formation in the tibia? A longitudinal study using PET/CT. *Clin Orthop Relat Res* 2017;475:1486-98. <https://doi.org/10.1007/s11999-017-5250-8>.
15. Blake GM, Puri T, Siddique M, et al. Site specific measurements of bone formation using [(18)F] sodium fluoride PET/CT. *Quant Imaging Med Surg* 2018;8:47-59. <https://doi.org/10.21037/qims.2018.01.02>.
16. Rhodes S, Batzdorf A, Sorci O, et al. Assessment of femoral neck bone metabolism using (18)F-sodium fluoride PET/CT imaging. *Bone* 2020;136:115351. <https://doi.org/10.1016/j.bone.2020.115351>.
17. Rajapakse CS, Gupta N, Evans M, et al. Influence of bone lesion location on femoral bone strength assessed by MRI-based finite-element modeling. *Bone* 2019;122:209-17. <https://doi.org/10.1016/j.bone.2019.03.005>.
18. Oldan JD, Hawkins AS, Chin BB. (18)F sodium fluoride PET/CT in patients with prostate cancer: quantification of normal tissues, benign degenerative lesions, and malignant lesions. *World J Nucl Med* 2016;15:102-8. <https://doi.org/10.4103/1450-1147.172301>.
19. Siddique M, Frost ML, Blake GM, et al. The precision and sensitivity of (18)F-fluoride PET for measuring regional bone metabolism: a comparison of quantification methods. *J Nucl Med* 2011;52:1748-55. <https://doi.org/10.2967/jnumed.111.093195>.
20. Brenner W, Vernon C, Muzi M, et al. Comparison of different quantitative approaches to 18F-fluoride PET scans. *J Nucl Med* 2004;45:1493-500.
21. Puri T, Blake GM, Frost ML, et al. Comparison of six quantitative methods for the measurement of bone turnover at the hip and lumbar spine using 18F-fluoride PET-CT. *Nucl Med Commun* 2012;33:597-606. <https://doi.org/10.1097/MNM.0b013e3283512adb>.
22. Schreiber JJ, Anderson PA, Rosas HG, et al. Hounsfield units for assessing bone mineral density and strength: a tool for osteoporosis management. *J Bone Joint Surg Am* 2011;93:1057-63. <https://doi.org/10.2106/jbjs.J.00160>.
23. Gausden EB, Nwachukwu BU, Schreiber JJ, et al. Opportunistic use of CT imaging for osteoporosis screening and bone density assessment: a qualitative systematic review. *J Bone Joint Surg Am* 2017;99:1580-90. <https://doi.org/10.2106/jbjs.16.00749>.
24. Lee S, Chung CK, Oh SH, et al. Correlation between bone mineral density measured by dual-energy X-ray absorptiometry and hounsfield units measured by diagnostic CT in lumbar spine. *J Korean Neurosurg Soc* 2013;54:384-9. <https://doi.org/10.3340/jkns.2013.54.5.384>.
25. Romme EA, Murchison JT, Phang KF, et al. Bone attenuation on routine chest CT correlates with bone mineral density on DXA in patients with COPD. *J Bone Miner Res* 2012;27:2338-43. <https://doi.org/10.1002/jbmr.1678>.

26. Shahinian VB, Kuo YF, Freeman JL, et al. Risk of fracture after androgen deprivation for prostate cancer. *N Engl J Med* 2005;352:154-64. <https://doi.org/10.1056/NEJMoa041943>.
27. Soares CBG, Araújo ID, Pádua BJ, et al. Pathological fracture after radiotherapy: systematic review of literature. *Rev Assoc Med Bras (1992)* 2019;65:902-8. <https://doi.org/10.1590/1806-9282.65.6.902>.
28. Patel U, Skingle S, Campbell GA, et al. Clinical profile of acute vertebral compression fractures in osteoporosis. *Br J Rheumatol* 1991;30:418-21. <https://doi.org/10.1093/rheumatology/30.6.418>.
29. Amelot A, Terrier LM, Cristini J, et al. Approaching spinal metastases spread profile. *Surg Oncol* 2019;31:61-6. <https://doi.org/10.1016/j.suronc.2019.08.007>.
30. Wang C, Shen Y. Study on the distribution features of bone metastases in prostate cancer. *Nucl Med Commun* 2012; 33:379-83. <https://doi.org/10.1097/MNM.0b013e3283504528>.
31. Tzolos E, Dweck MR. (18)F-sodium fluoride ((18)F-NaF) for imaging microcalcification activity in the cardiovascular system. *Arterioscler Thromb Vasc Biol* 2020;40:1620-6. <https://doi.org/10.1161/atvbaha.120.313785>.
32. Sorci O, Batzdorf AS, Mayer M, et al. (18)F-sodium fluoride PET/CT provides prognostic clarity compared to calcium and Framingham risk scoring when addressing whole-heart arterial calcification. *Eur J Nucl Med Mol Imaging* 2020;47:1678-87. <https://doi.org/10.1007/s00259-019-04590-3>.

